Mutations in the coordination spheres of T1 Cu affect Cu^{2+}-activation of the laccase from *Thermus thermophilus*

Romain Clément[1], Xie Wang[2], Frédéric Biaso[1], Marianne Ilbert[1], Ievgen Mazurenko[1], Elisabeth Lojou[1*]

[1] Aix Marseille Univ, CNRS, BIP, Bioénergétique et Ingénierie des Protéines, UMR 7281, 31, chemin Joseph Aiguier, CS 70071 13402 Marseille cedex 09, France

[2] Laboratoire de Chimie Physique et Microbiologie pour les Matériaux et l'Environnement, Université de Lorraine, CNRS, LCPME UMR 7564, 405, rue de Vandoeuvre, 54600 Villers-lès-Nancy, France

Abstract

Thermus thermophilus laccase belongs to the sub-class of multicopper oxidases that is activated by the extra binding of copper to a methionine-rich domain allowing an electron pathway from the substrate to the conventional first electron acceptor, the T1 Cu. In this work, two key amino acid residues in the 1st and 2nd coordination spheres of T1 Cu are mutated in view of tuning their redox potential and investigating their influence on copper-related activity. Evolution of the kinetic parameters after copper addition highlights that both mutations play a key role influencing the enzymatic activity in distinct unexpected ways. These results clearly indicate that the methionine rich domain is not the only actor in the cuprous oxidase activity of CueO-like enzymes.

Keywords: Laccase; Directed mutagenesis; Copper activation; Spectroscopies; Electrochemistry

1. Introduction

Laccases (LACs) belong to the multicopper oxidases (MCOs) family found in a multitude of organisms and mainly in fungal and bacterial kingdoms [1-3]. They couple the four-electron reduction of molecular oxygen to water with the oxidation of a wide variety of phenolic or non-phenolic molecules. Thanks to these catalytic properties, LACs are prone to be used in biotechnological applications such as in bioremediation, decolorization, and detoxification [4, 5]. They are also envisioned as biocatalysts at the cathode of enzymatic fuel cells (EFCs), the anode being fueled with sugars, alcohol or dihydrogen (H_2), to give a few relevant examples [6–8]. In our laboratory, we particularly highlighted that the discovery in the biodiversity of redox enzymes presenting new outstanding properties may improve the performances of EFCs [9, 10]. In such EFCs, the cathodic enzymatic reaction limits the whole device. Issues in the communication of the enzyme with the electrode, inappropriate redox potential or chloride sensitivity impose to search for more efficient redox enzymes for O_2 reduction [8, 11].

Two main strategies can be undertaken to obtain more efficient LACs for biotechnology. As just noticed above, the first method is to find LACs in diverse natural environments presenting suitable catalytic properties. It is well known that LACs present low to high redox potentials for O_2 reduction, which are microorganism dependent [3, 6]. Otherwise, LACs from halophiles or thermophiles are reported to present strong resistance to chloride inhibition or to be thermostable [12-14]. The second method is to use gene modification techniques like directed mutagenesis or directed evolution by random mutagenesis to improve LAC properties [15-20]. Directed evolution allowed improved decolorization process, substrate specificity, pH stability, chloride tolerance or redox properties.

Although many previous works discussed the effect of single or multiple mutations on properties of different LACs, either bacterial or fungal, LACs from the bacterium *Thermus thermophilus* have been the subject of only rare reports. *T. thermophilus* LACs do deserve more attention not only for their biotechnological interest because of stability at high temperatures, but also for the presence of an unusual methionine (M) rich loop covering the T1 Cu site, where substrates bind in classical MCOs. Actually, *T. thermophilus* LACs belong to the MCO group including the copper efflux oxidase CueO of *Escherichia coli* that are activated by addition of exogenous copper [21-23]. In addition to classical T1 Cu and T2/T3 Cu sites, these enzymes can fix additional labile coppers in the M rich domain allowing the electron transfer from the substrate to the T1 Cu [24-29]. We recently performed an in-depth electrochemical study of the intra- and inter-electron transfers using the LAC of *Thermus thermophilus* HB27 (Tt-LAC) immobilized on different electrodes [23]. We demonstrated a Cu^{2+}-related bioelectrocatalytic process proposed to be linked to the binding of additional Cu^{+} to the M-rich domain (denoted thereafter sCu), and which induces a new electron transfer pathway to the T2/T3 trinuclear

Cu active site. Although the exact mechanism is not fully understood *in vivo*, we proposed from the electrochemical study that higher specificity of M-sites for Cu^{+} than Cu^{2+} leads to the increase of the redox potential of bound Cu^{2+}/Cu^{+} couple, which becomes able to withdraw electrons from the substrate and pass them further to T1 Cu. This new electron transfer pathway would correspond to a cuprous oxidase activity of Tt-LAC, an activity which is largely understudied in the literature although crucial for copper detoxification.

To get further insight in the electron transfer pathway involved in *Thermus thermophilus* HB27, we tuned in this work Tt-LAC catalytic properties by directed mutagenesis of two relevant M residues in the coordination spheres of the T1 Cu site. Our aim was to study the potential impact of these mutations that are expected to affect the T1 Cu redox potential on activation of the enzyme by Cu^{2+}. In particular, M455, the axial ligand of T1 Cu, was replaced by leucine (L) and phenylalanine (F), as this mutation was previously shown in classical MCOs to induce an increase in the T1 Cu redox potential [30, 31]. M456 was mutated to alanine (A) recognized as a conserved residue in high potential LACs. Tt-LAC wild type and mutants were compared by a multidisciplinary approach combining enzymology, UV-Vis, circular dichroism (CD) and electron paramagnetic resonance (EPR) spectroscopies, as well as electrochemistry to determine how mutations affect the properties of the enzyme. Interestingly, our work underlines modifications of the Cu^{2+} activation process in the two mutants in comparison to the wild type Tt-LAC. Evolution of the kinetic parameters after copper addition highlights that both mutations play a key role influencing the enzymatic activity in distinct unexpected ways.

2. Materials and methods

2.1. Strains, media, and chemicals

E. coli DH5α and *E. coli* Origami™ 2(DE3) (Merck Millipore, Burlington, USA) were used for plasmid amplification and heterologous recombinant LAC protein expression, respectively. pET-21 b (Addgene, Cambridge, USA) was used for gene expression of Tt-LAC WT and mutants. *E. coli* strains were grown in LB media (Merck, Darmstadt, Germany) with selectable antibiotics. High purity chemical products were from Sigma-Aldrich (Merck, Darmstadt, Germany).

2.2. Vector construction

The gene encoding Tt-LAC (gene accession number: AAS81712.1) was inserted in the plasmid pET-21 b (ampicillin resistance) for its use in *E. coli* Origami™ 2(DE3) which is resistant to kanamycin and tetracycline. PET-21 b was linearized with primers PRC3 and PRC4 (Table S1) and the gene encoding for Tt-LAC was amplified with primers PRC1 and PRC2. Ligation was performed by SLIC methods previously described [32]. Site directed mutagenesis was performed with the QuikChange® Site-

Directed Mutagenesis Kit (Stratagene, San Diego, USA) with primers described in Table S1. Plasmids were transformed in *E. coli* DH5α strain and subsequently in *E. coli* Origami™ 2(DE3). Strains used for protein expression are described in Table S2. Plasmids were sequenced by Genewiz (Leipzig, Germany).

2.3. Protein expression and purification

An overnight culture of the strain RC024 for Tt-LAC expression or its derived mutants (strains RC045, RC046, RC047 and RC079; Table S2) was used to inoculate fresh LB medium (1/200 dilution). Cells were grown at 37°C in aerobic condition up to 0.6 absorbance at 600 nm. 500 µM IPTG for the gene induction and 500 µM $CuSO_4$ were added in the medium and the temperature was decreased to 22°C. Protein expression was performed during 24 hours in aerobic condition followed by 24 hours in anaerobic condition. Cells were harvested by centrifugation at 7200 g and frozen at -80°C.

Cell pellet was resuspended at 4°C in 50 mM sodium phosphate buffer pH 7.4 containing 500 mM NaCl and 10 mM imidazole (Buffer 1). Protease inhibitor, lysozyme, and DNase were added. Cells were broken by sonication during 1 minute, 5 times at 4°C (Sonic & Material Inc, Bioblock, Danbury, USA). The crude extract was centrifuged at 10 500 g during 30 minutes and then at 140 000 g during 30 minutes. Tt-LAC proteins or Tt-LAC mutants were purified from the supernatant by His-Trap HP 1 ml column (GE Healthcare, Chicago, USA) with steps at 50 mM, 250 mM and 500 mM imidazole. Proteins were eluted at 250 mM imidazole, dialyzed against 100 mM sodium phosphate buffer pH 7.4 (Buffer 2) with dialysis tubing (12-15 kDa pore size, Medicell Membrane Ltd, London, UK) overnight, and then concentrated with centrifugal filter 30 kDa (Vivaspin®, Sartorius, Göttingen, Germany). SDS PAGE gel was performed to check protein purity by the loading of 5 µg of purified proteins. Pure proteins were aliquoted, frozen in liquid nitrogen and stored at -80°C. Samples were dialyzed against desired buffers overnight at 4°C to change the pH before use when needed.

2.4. Absorption spectra

Protein absorption spectra were recorded with 50 µM of protein in 50 mM acetate buffer pH 5. Spectra were recorded in the range between 900 and 200 nm (Cary 50 UV-Vis, Palo Alto, USA).

2.5. Enzymatic assays

Enzymatic assays were performed at 30°C by measuring the absorption at 420 nm using a spectrophotometer microplate reader (Spark 10M, Tecan, Männedorf, Swiss). 2,2'-azino-bis(3-ethylbenzothiazoline-6-sulphonique) (ABTS) was used as the electron donor. Three replicates were performed. Enzymatic kinetic parameters were calculated by Sigma-Plot (Systat Software Inc., San Jose, USA) according to Michaelis constant with one site saturation:

$$V_i = \frac{V_{max} \times [S]_0}{K_M + [S]_0},$$

where V_i = initial speed, V_{max} = maximal initial speed, K_M = affinity and $[S]_0$ = ABTS concentration.

The Cu^{2+} activation ($K_{1/2}$) for the WT and M456A, or the Cu^{2+} half maximal inhibitory concentration (K_{IC50}) for M455L and M455F were calculated with the respective hyperbolic equations:

$$V_i = Act_{Cu0} + \frac{V_{max} \times [Cu^{2+}]_0}{K_{1/2} + [Cu^{2+}]_0} \quad - \quad for\ activation,$$

$$V_i = \frac{V_{max} \times K_{IC50}}{K_{IC50} + [Cu^{2+}]_0} \quad - \quad for\ inhibition,$$

where Act_{Cu0} = activity without $CuSO_4$, $[Cu^{2+}]_0$ = $CuSO_4$ concentration, and K_{iC50} = Cu^{2+} inhibition constant.

The kinetic data were obtained in air-saturated conditions. Considering the value of K_M for O_2 also measured in this work (Fig. S5), all the Michaelis constant values are apparent ones K_M^{app}.

2.6. Bioinformatics

Pymol (Schrödinger, New-York, USA) was used to draw protein structures and to measure distances. Phyre2 [33] was used to model protein structure of mutants and Clustalw Omega to perform alignment.

2.7. Optical Emission Spectrometry, Inductively Coupled Plasma analysis (ICP-OES)

Copper content in enzymes was determined using an iCAP-7000 ICP-OES analyzer. 50 µg of proteins (wild-type or mutants) were treated. 2 biological replicates were analyzed as given in Table 1.

2.8. Electron paramagnetic resonance spectroscopy (EPR)

X-band CW EPR spectra were measured at 60 K on a Bruker EleXsys E500 spectrometer equipped with an ER4102ST standard rectangular Bruker EPR cavity fitted to an Oxford Instruments helium flow cryostat. Numerical simulations of EPR spectra were performed using the EasySpin package (release 5.0.12) on Matlab (The MathWorks, Inc., US) [34].

2.9. Circular dichroism (CD) spectroscopy

5 μM of proteins in 50 mM acetate buffer pH 5 were analyzed by far-UV CD spectroscopy using a Jasco J-715 spectropolarimeter at 298 K in a 1mm path length cell. The average of five accumulating scans was performed.

2.10. Electrochemistry

A small aliquot (typically 5 μl) of 10 μM purified enzymes, either WT or mutants was deposited on a graphite electrode (geometric surface area 0.07 cm^2). Unless otherwise specified, the graphite electrode was modified by a thin film of carbon nanofibers (CNF), to favor protein adsorption and electrical communication with the electrode. Properties of CNFs were described previously [35]. After optimization, 2 layers of CNF (4 mg/ml) were dried on the electrode surface. The adsorption of the enzyme on the electrode surface was made at 4°C during 15 min. Then the bioelectrode was gently washed with buffer to remove loosely adsorbed proteins. Cyclic voltammetry (CV) was performed at 25°C in a standard 3-electrode cell using a potentiostat from Eg&G instrument (model 263A) controlled by Echem software. Ag/AgCl (NaCl sat.) and Pt-wire were used as reference and auxiliary electrodes, respectively. All potentials are quoted vs NHE reference electrode by adding 210 mV to the measured potential. 50 mM acetate buffer pH 5.6 was used as the electrolyte.

3. Results and Discussion

3.1. Directed mutations

We recently determined the onset potential for O_2 reduction by Tt-LAC using direct electrochemistry on carbon nanotube-modified electrodes [23]. We showed that Tt-LAC belongs to the middle-low redox potential LAC family and reduces O_2 at a potential of +650 mV vs NHE at pH 5. The axial ligand of T1 Cu is recognized to play a key role in the geometry of the Cu site, hence in its redox potential. In Tt-LAC, the axial ligand is M at position 455. Generally, LACs with M as axial ligand of T1 Cu present low redox potential. ClustalW alignment performed with laccases sorted by potential [16] is shown in Fig. S1. It clearly appears that more hydrophobic L or phenylalanine amino acid residues instead of M as T1 Cu axial ligand favor high redox potentials. After sequence comparison between high redox and low redox LACs (Fig. S1), we also observed that most high redox potential LACs have A residue next to their axial ligand. We thus mutated M455 by L (M455L) and M456 by A (M456A) that we expect to play a major role. We also constructed M455F and the double mutant (M455L-M456A) for further kinetic analysis (Fig. S2 and S3, respectively). Tt-LAC WT and studied mutants are illustrated on the protein sequence in Fig. 1A and in the protein crystal structure in Fig. 1B. As we know that Cu^{2+} exogenous addition strongly influences Tt-LAC WT activity, the effect of Cu^{2+} on the structural and kinetic properties of these mutants will be especially investigated.

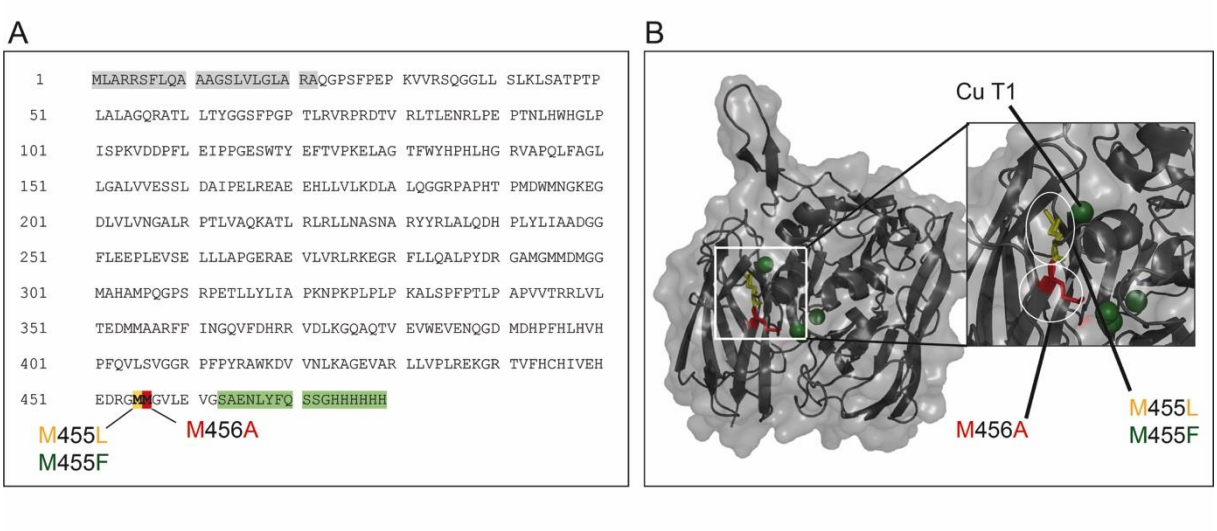


Fig. 1. *(A) Tt-LAC protein sequence. Grey: signal sequence; green: histidine tag sequence. (B) Laccase of Thermus thermophilus HB27 crystallographic structure [22] and zoom on the T1 copper center. Yellow: mutated M455 axial amino acid; red: mutated M456 amino acid. The reference of the pdb structure is 2XU9 from Serrano-Posada et al [22].*

3.2. Structural analysis and copper content of Tt-LAC WT and M455L and M456A mutants

Protein was produced and purified following previous methods developed to produce *Bacillus pumilus* and *Bacillus subtilis* BODs [36-38]. About 5 mg of LAC per liter of bacterium culture was produced. LAC purity was confirmed by SDS PAGE colored by Coomassie blue (Fig. 2A).

CD analysis was carried out to evaluate potential structural changes between Tt-LAC WT and studied mutants (Fig. 2B). All spectra superimposed, showing that mutations did not affect protein secondary structure. As Tt-LAC is known to be activated by Cu^{2+} addition, we also recorded CD spectra of WT and mutants in the presence of 50 µM Cu^{2+} in solution. No change in the spectra hence in the secondary structure can be detected (Fig. 2B). In addition, Phyre2 was used to model Tt-LAC mutant structures. As can be seen in Table S3, distances of the T1 Cu with its ligands, i.e. cysteine, histidine and axial amino acid are conserved.

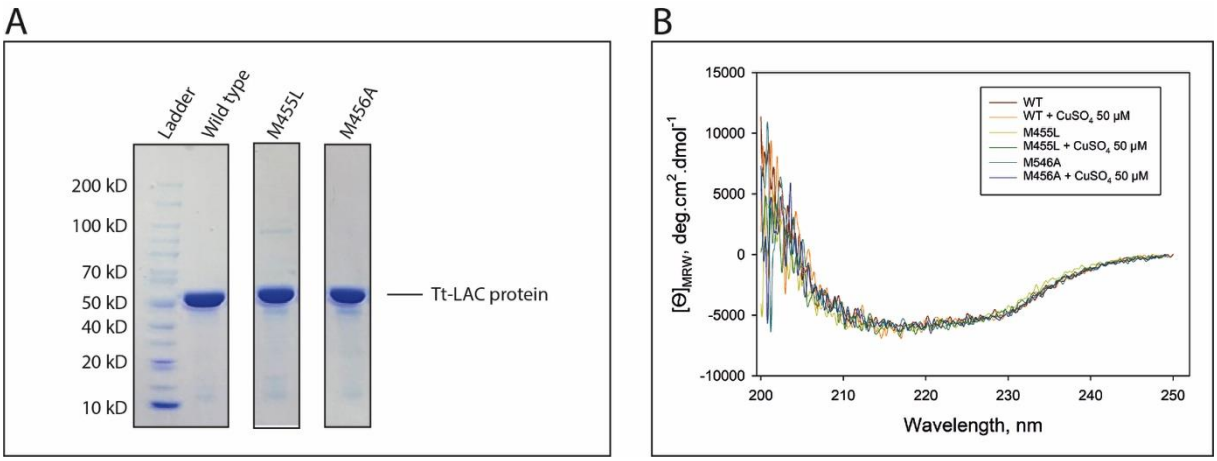


Fig. 2. *(A) Purified laccase of Thermus thermophilus HB27 WT and mutants after migration on SDS-PAGE 4-15%. 5 µg of proteins were loaded. (B) Circular dichroism analysis in acetate buffer pH 5, without or with 50 µM $CuSO_4$.*

To estimate the copper incorporation rate in LAC proteins, quantification by ICP with two biological replicates was performed. Incorporation of 3-4 copper atoms was observed for the WT as well as for M455L and M456A (Table 1). These data suggest that we successfully maturated LAC proteins even though a small population of proteins might not fully contain the expected 4 Cu atoms.

Table 1. *Laccase of Thermus thermophilus WT and mutants' copper content and kinetic parameters in solution*

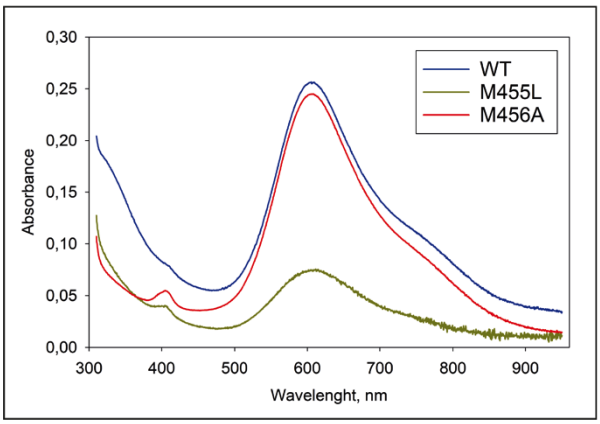
			Without $CuSO_4$ (30°C, pH 5)			With $CuSO_4$ 500 µM (30°C, pH 5)		
	[Cu]/mol of protein (mol)	$K_{1/2}$ [$CuSO_4$] activation (µM, pH 5)	k_{cat} (s^{-1})	K_M^{app} (mM ABTS)	k_{cat}/K_M^{app} ($s^{-1}.M^{-1}$)	k_{cat} (s^{-1})	K_M^{app} (mM ABTS)	k_{cat}/K_M^{app} ($s^{-1}.M^{-1}$)
WT	3.30 ± 0.05 3.57 ± 0.03	117 ± 8	0.25 ± 0.004	2.937 ± 0.148	85.1	0.69 ± 0.017	1.580 ± 0.139	436.7
M455L	3.75 ± 0.03 3.84 ± 0.42	-	0.16 ± 0.005	0.307 ± 0.047	521.2	-	-	-
M456A	3.54 ± 0.01 3.86 ± 0.33	84 ± 11	-	-	-	0.15 ± 0.003	2.327 ± 0.166	64.5

It was previously reported a sequential incorporation of copper in CueO, the T1 being first completed, followed by T2 and T3 upon protein incubation in increasing Cu^{2+} concentrations [39]. To better analyze the presence/absence of the different LAC Cu centers, we further analyzed them by spectroscopies. UV-Vis spectra were first recorded for Tt-Lac WT and mutants (Fig. 3A). No modification of the UV-Vis spectra was observed after treatment with potassium hexachloroiridate, demonstrating that bound coppers are in the Cu^{2+} state. As expected, a band at 607 nm that corresponds to the S(Cys)$\pi \rightarrow$Cu(II)

charge transfer at the T1 Cu site is observed for the Tt-LAC WT [21]. UV-Vis spectra of M456A and M455L display a similar band, suggesting that T1 Cu conserves its geometry in the mutants. In comparison with the WT UV-Vis spectrum, the magnitude of the absorbance peak for T1 Cu site in M456A is very similar to the WT, while M455L mutant spectrum shows a lower magnitude peak, being 30% less than that of the WT. Absorbance peak decrease at 607 nm suggests some depletion of T1 Cu site in M455L mutant. It is noticeable however, that our protocol for copper incorporation is much more efficient than the protocol recently used by Zhu et al. [31]. T2/T3 active site is attested by a weak-defined band at 330 nm for Tt LAC WT, induced by a bridging hydroxo ligand between T3 coppers. This band is less intense with the mutants. Such observation can be attributed to a population of LAC depleted in T3 Cu. Another explanation might be associated to the presence of an oxygen bound to the T3 sites rather than the typical hydroxo bridge, as demonstrated previously in CotA LAC mutants [40].

EPR spectroscopy provides additional information since T1 and T2 Cu sites present specific signatures. Fig. 3B shows the EPR spectra of the WT enzyme and M456A and M455L mutants. Each spectrum corresponds to the sum of typical T1 and T2 Cu signals. The simulation of EPR spectra reveals that three kinds of Cu(II) signals are present for which the g- and A(Cu) parameters correspond to one T1 site and two different T2 sites (noted T2 and T2') (Table S4). For all samples, the g and A(Cu) parameters are in the range of those reported for LACs [41]. Interestingly, small splits are observed in the perpendicular region which correspond to two ^{14}N nuclei with a coupling constant of about 14.10^{-4} cm^{-1}. Such nitrogen couplings are sometimes observed in copper centers, depending on the linewidth and the covalency of metal-ligand bonds and the magnitude of this type of coupling is typically in the range $10\text{-}15.10^{-4}$ cm^{-1} [42]. Considering that intensity of these peaks follows the same behavior than those of T2 Cu signal, these superhyperfine interactions probably arise from the nitrogen of the two coordinated histidine residues in the Cu T2 site. Mutations only slightly affect the magnetic parameters of T1 and T2 Cu sites.

A



B

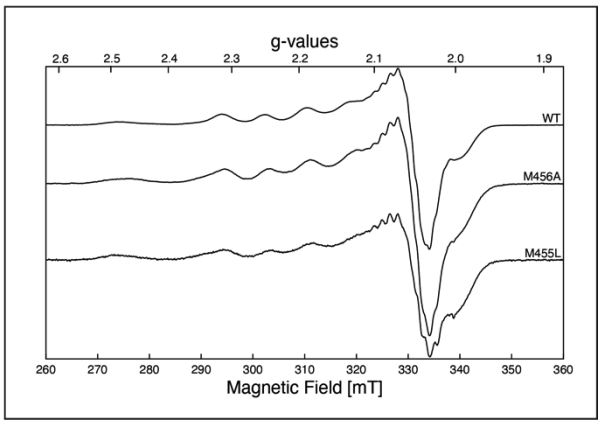


Fig. 3. *(A) Tt-LAC WT and mutants UV/visible spectra in 50 mM acetate buffer at pH 5. (B) Frozen solution EPR spectra of Tt-LAC WT and mutants in 100 mM sodium phosphate buffer (pH 7.4). Intensity of the EPR spectra are normalized with respect to the protein concentration. Acquisition parameters: T = 60 K, microwave power 4 mW, microwave frequency 9.481 GHz, modulation amplitude 0.5 mT.*

Durao et al. proposed that the T2 Cu site of LACs can have two kinds of signatures [40], depending on the presence of the T3 Cu site. For LACs for which the T3 Cu site is absent, the T2 Cu site exhibits an EPR spectrum different from that of fully loaded LACs. Considering the copper quantification by ICP-OES and UV-visible absorption spectroscopy, it is likely that Tt-LAC samples are constituted of two populations: a population of fully loaded protein with all T1, T2 and T3 copper sites and a second population of proteins which would be either depleted in Cu at the T3 site, or presenting alteration in T3 Cu coordination sphere. Thus, the T2' signal could be attributed to this population which is higher in the mutants compared to the WT, being respectively, 34%, 21% and 15% for M455L, M456A and WT, respectively (Table S4). Simulation weight parameters suggest however that the fully loaded protein represents the main population for all samples. Since the T1 Cu site is further away from the trinuclear site, its EPR signal is not affected by the T3 Cu site. The percentage of T1 Cu in Tt-LAC WT and mutants is in accordance with UV-Vis results, confirming a similar T1 Cu content in WT and M456A, while M455L contain around 50% less T1 Cu than the WT.

3.3. Effect of T1 Cu site mutation on onset potentials for O_2 reduction

Direct electrochemistry of Tt-LAC WT and mutants was performed on a graphite electrode modified by a film of carbon nanofibers (Fig. 4). In this configuration, the electrode can be considered as the substrate of the enzyme, being the electron donor. To succeed in an electron exchange between the enzyme and the electrochemical interface, one key factor is the distance between the electrode and the T1 Cu. In the case of Tt-Lac WT, in the presence of O_2, and in the absence of any diffusing redox mediator, a sigmoidal signal occurs, with a cathodic wave and no anodic counterpart, characteristic of the enzymatic reduction of O_2 by the immobilized enzyme. The onset for O_2 reduction is observed at 556 mV vs NHE and pH 5.6, in accordance with the redox potential of the T1 Cu [26]. Carbon nanofiber modification of the electrode allows to increase the enzyme loading on the electrode but also enables the orientation of the enzyme in a way that favors the direct electron transfer between the T1 Cu and the electrode. We previously demonstrated that positively charged interfaces were in favor of a direct wiring because of the presence of a negative area in the vicinity of the T1 Cu [23]. The carbon nanofibers used in the current work present a hydrophobic surface, suggesting that hydrophobic interaction should also play a key role in the efficient electrical wiring of the enzyme [35]. This is not unexpected as it was demonstrated that substrate-enzyme complex was mainly driven by hydrophobic

interactions [43]. The mutants were then adsorbed on the same carbon nanofiber-modified electrode. We were not able to get any electrochemical signal for M455F and the double mutant, most probably because of much lower enzymatic activity. M456A Tt-LAC mutant generates a catalytic signal for O_2 reduction at the same potential than the WT. The enhancement of the redox potential expected from sequence comparison is not obtained. It must be noted that the current is ten times lower than that obtained with the WT. For M455L Tt-LAC, the onset for O_2 reduction is shifted anodic to 650 mV vs NHE. This shift of almost 100 mV confirms the reported influence of leucine ligand against methionine to promote high T1 Cu redox potentials in various MCOs [31]. It was proposed that this anodic shift would be linked to the stabilization of the reduced state of Cu in the absence of methionine axial ligand. As can be seen in Fig. 4, a noticeable feature is that the catalytic current is even lower than the current recorded with M456A mutant, being around 30 times lower than the catalytic current measured with Tt-LAC WT.

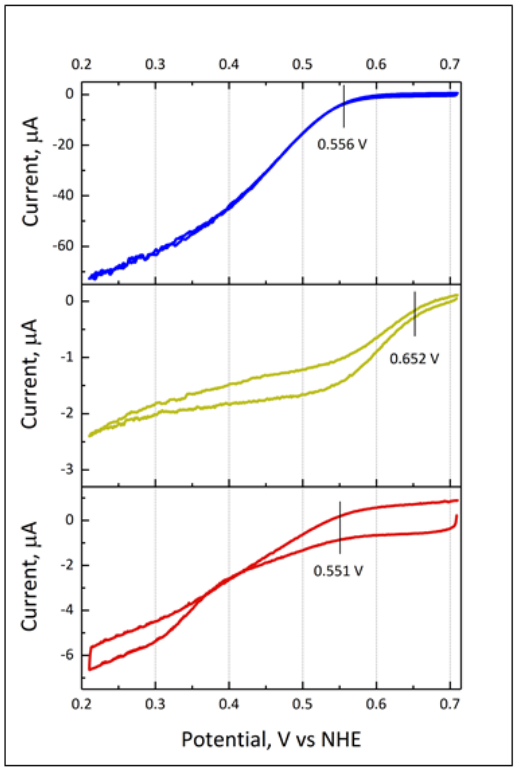


Fig. 4. *O_2 catalytic reduction by Tt-LAC WT (blue line), M455L (yellow line) and M456A (red line) mutants adsorbed on carbon nanofiber-modified graphite electrode. Observed onset redox potentials are shown by a vertical line. 50 mM acetate buffer pH 5.6, sweep rate 5 mV.s^{-1}.*

3.4. Mutation effect on Tt-LAC kinetics in solution

Enzyme activities were then measured in solution with Tt-LAC WT and mutants using ABTS as the electron donor (Fig. 5). All the deduced kinetic parameters are gathered in Table 1 for WT, M455L and M456A. Fig S2 and S3 show the additional kinetic data for M455F and M455L-M456A respectively. While WT Tt-LAC presents a k_{cat} of 0.25 s^{-1}, no activity was recorded with M456A. The same behavior was observed with the double mutant. M455L and M455F were active for ABTS oxidation, but k_{cat} was negatively affected, being 64% of WT for M455L, and only 12% of WT for M455F.

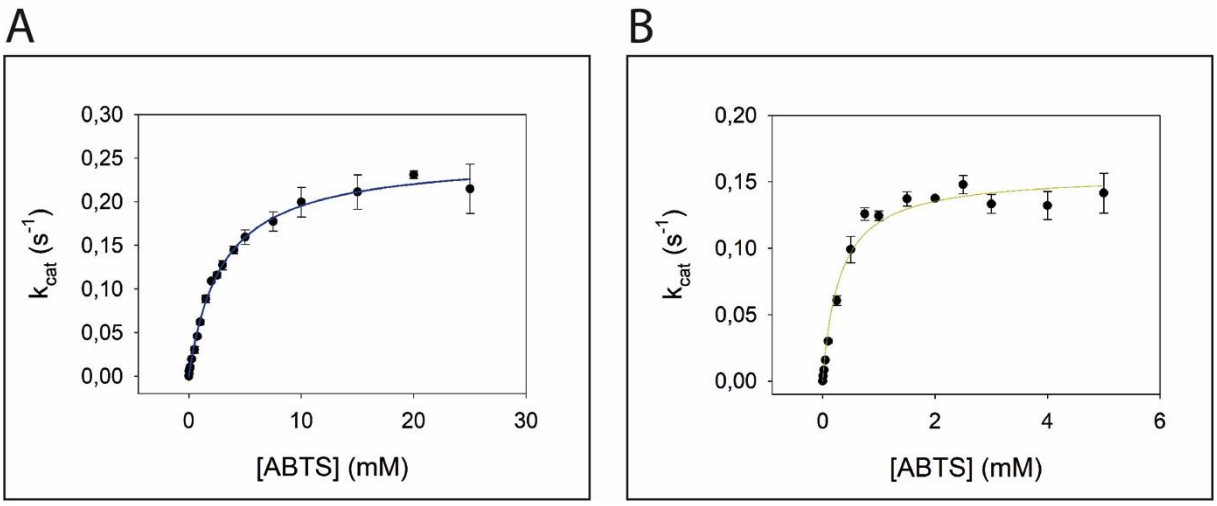


Fig. 5. *Enzymatic assays in solution of (A) wild type Tt laccase and (B) M455L mutant. Assays were performed with ABTS at pH 5 in 50 mM acetate buffer.*

From CD and UV-Vis data, we concluded that the secondary structure and T1 Cu content is preserved in M456A. UV-Vis and EPR measurements suggest however that T3 Cu site is modified compared to the WT. If the major alteration denoted by spectroscopies is the depletion of T3 Cu in some proteins, these latter will obviously have no activities. However, EPR spectra clearly shows that this is not a major part of the proteins, and electrochemistry proved that at least a population of enzymes is active. The lack of activity of M456A with ABTS must thus have another origin. Actually, according to Marcus theory, the rate of electron transfer k_{ET}, which controls k_{cat}, is not only dependent on the redox potential and on the distance between the donor and acceptor, but also on the reorganization energy [44]. It was demonstrated by Durao et al. [40] that mutation of Ile into A in the T1 Cu vicinity of CotA LAC increases the accessibility of the T1 Cu site, so that a solvent molecule could interact with the Cu site. It was proposed that this alteration would require an increase in the reorganization energy, resulting in a lower electron transfer rate, thus a lower k_{cat}. The replacement of M residue by the smaller amino acid residue A in the current work could have the same effect, modifying the accessibility of the T1 Cu as well. Moreover, M456A can be electrically wired, being active for the electrocatalytic reduction of O_2 when an electrode is replacing ABTS as the substrate, as shown in

Figure 4. All these features are in favor of a modification of ABTS affinity compared to WT Tt Lac by modifying the second sphere of T1 Cu coordination.

Concerning the activity of M455L and M455F, negative alteration of the k_{cat} after T1 Cu axial amino acid mutation seems to be common [30, 45]. As an example, Durao et al. replaced axial M by L or F in the LAC of *Bacillus subtilis* [45]. k_{cat} was negatively altered by both mutations, and redox potentials were increased by 100 mV and 60 mV, respectively, in agreement with our finding. k_{cat} decrease can arise in part from the T1 Cu content of the mutant as determined by UV-Vis and EPR spectroscopies in the current work. Increase in the redox potential for M455L demonstrated here by electrochemistry, can also directly impact k_{cat}. Besides ABTS oxidation by T1 Cu, k_{cat} combines all further steps of electron transfer, i.e. intramolecular electron transfer T1->T2/T3 as well as oxygen binding, reduction, and release on the trinuclear cluster. Assuming that the trinuclear cluster was not impacted by T1 ligand mutation, decrease of k_{cat} might be explained either by the decreased rate of ABTS oxidation by T1 or by the decreased rate of intramolecular electron transfer T1->T2/T3 induced by the increased T1 Cu potential.

In contrast with Durao finding [45], a significant decrease of the K_M^{app} for M455L and M455F, being respectively 10-fold and 28-fold less than the WT is recorded. Two main phenomena can explain this strong K_M^{app}. decrease. A first explanation arises from the quasi-steady-state derivation of the Michaelis-Menten equation suggesting that for the classical simplified enzymatic equation:

$$E + S \underset{k_r}{\overset{k_f}{\rightleftharpoons}} ES \overset{k_{cat}}{\rightharpoonup} E + P$$

K_M^{app} can be represented as $K_M^{app} = \frac{k_r + k_{cat}}{k_f}$ instead of $K_M^{app} = \frac{k_r}{k_f} = K_D$ in equilibrium conditions. Thus, decrease of K_M^{app} may be associated not only with K_D decrease but with k_{cat} decrease while K_D remains unchanged. As mentioned above, k_{cat} decrease was observed for the mutants confirming this hypothesis. An alternative explanation for the low K_M^{app} of M455L and M455F would be an increased affinity for ABTS. Indeed, molecular dynamic simulation of the binding of ABTS to Tt-LAC highlighted that hydrophobicity was the main driving force of the substrate-enzyme complex formation [37]. Although M455 is part of the first coordination sphere of T1 Cu and is thus not directly involved into ABTS binding on the enzyme surface, mutation of M455 by leucine or phenylalanine may enhance the hydrophobicity of the substrate cavity.

3.5. Impact of Tt-LAC mutation on Cu^{2+} activation

Tt-LAC belongs to the CueO LAC group as classified by Solano et al. [46] that presents a M rich region

acting as a lid covering T1 Cu site that may hamper ABTS access. This region can bind a labile copper (sCu) that allows the activation of the enzyme [22]. The activation is initiated by Cu^{2+} addition in solution, higher specificity of M-sites for Cu^{+} than Cu^{2+} [26] leading to the increase of the redox potential of bound Cu^{2+}/Cu^{+} couple, which becomes able to withdraw electrons from the substrate and pass them further to T1 Cu [23, 25]. It must be noted, that the Cu^{2+}-related activation process cannot be linked to the incorporation of copper in some copper-depleted T1, T2 or T3 sites, since the activation process occurred even with a fully metallated protein [39]. However, the mechanism behind this activation process is not fully understood. To get new insight in the Cu^{2+}-activation process, we thus determined the kinetic parameters of WT and mutants in the presence of $500\ \mu M$ $CuSO_4$ in solution (Table 1). Fig. 6 shows the evolution of activity towards ABTS as a function of $CuSO_4$ concentration in solution. For Tt-LAC WT, $CuSO_4$ activation was similar to results described previously [21,23].

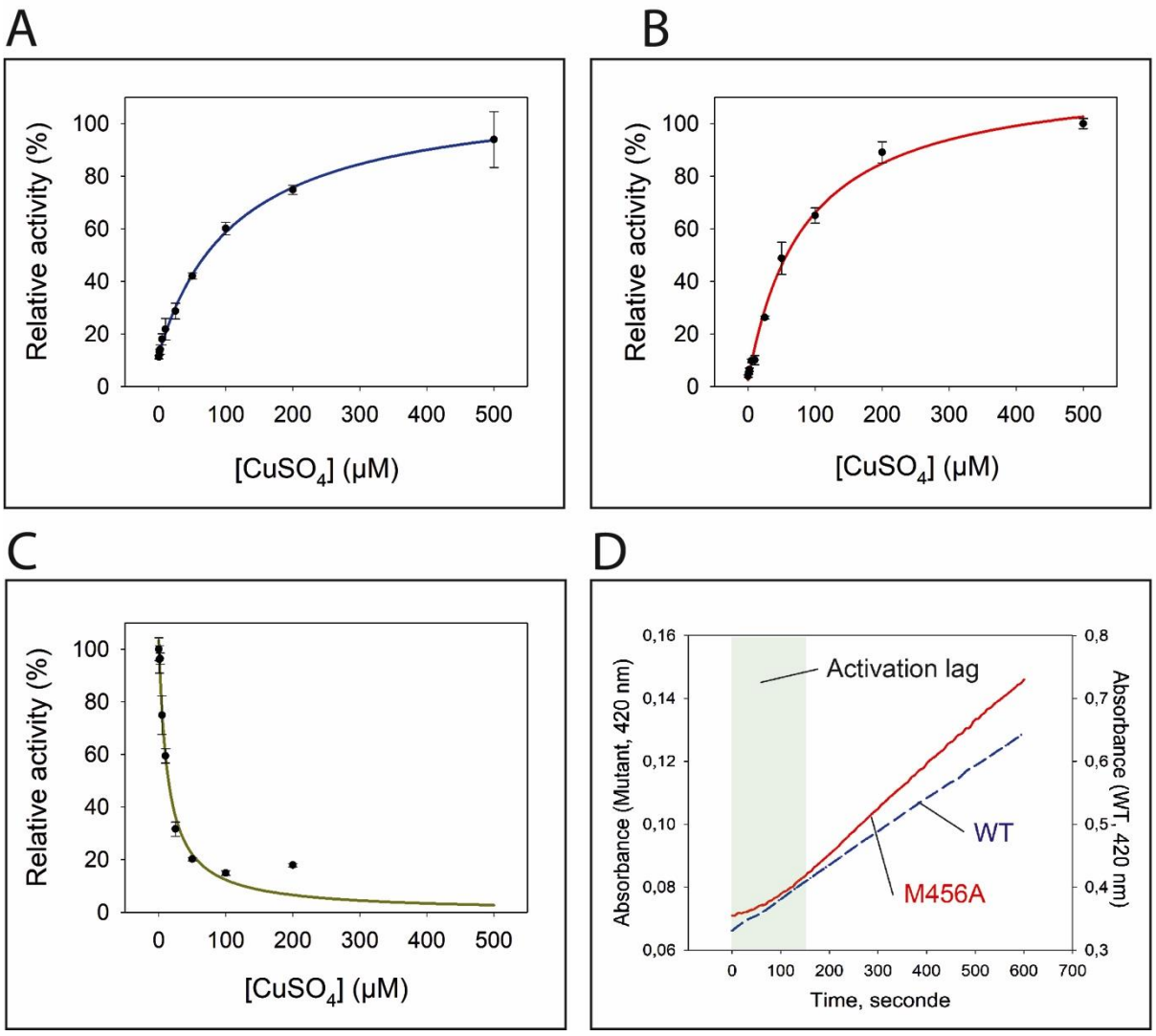


Fig. 6. *Copper activation/inhibition of the WT Tt-LAC and mutants. Activity was measured with 1 mM ABTS. (A)*

WT Tt-LAC; (B) M456A mutant; (C) M455L mutant. (D) shows the lag induced by $CuSO_4$ addition in M456A (red) in comparison to WT (blue).

An instantaneous activation by Cu^{2+} addition was observed with a $K_{1/2}$ of 117 ± 8 µM of $CuSO_4$ (Table 1 and Fig. 6A) although the enzyme had a non-negligible activity without additional copper. k_{cat} was 2.9-fold higher in the presence of 500 µM $CuSO_4$ and the affinity (K_M^{app}) was lower for ABTS (1.9-fold) than in the absence of $CuSO_4$. Notable different behaviors were observed with mutants compared to Tt-LAC WT upon copper addition (Fig. 6). Interestingly, Tt-LAC M456A becomes active with the addition of $CuSO_4$ displaying a $K_{1/2}$ of 84 ± 11 µM (Table 2, Fig. 6B). Fig. 7 underlines the M456A activation by 500 µM $CuSO_4$ in comparison with the WT. A k_{cat} of 0.15 ± 0.003 s^{-1} is calculated for M456A after $CuSO_4$ addition. K_M^{app} is 1.5-fold higher than for WT Tt-LAC, underlining again a low ABTS affinity. A similar behavior is observed with the double mutant, with a very low k_{cat} value however (Fig.S3). In this mutant, $K_{1/2}$ is close to 9 µM, at least ten times lower than in the case of WT or M456A.

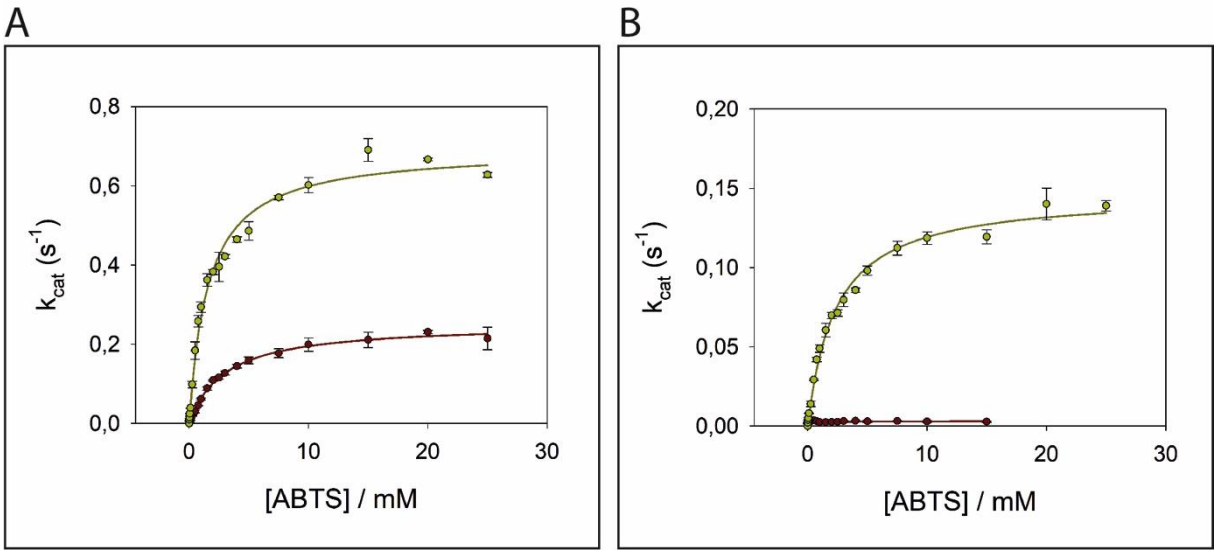


Fig. 7. *WT (A) and M456A mutant (B) activity with ABTS, with (dark yellow circles and lines) and without (dark red circles and lines) Cu^{2+} addition (500 µM) in acetate buffer 50 mM at pH 5.*

A completely different situation is observed with M455L. For this mutant, addition of $CuSO_4$ induces the inhibition of the activity with a K_{iC50} of 12.8 µM (Fig. 6C). Inhibition is also observed for M455F (K_{iC50} = 4.8 ± 0.5 µM; Fig. S2). Electrochemical experiments performed with WT, M456A and M455L immobilized on carbon electrodes, confirm the activation or inhibition process as a function of the protein used. Tt LAC WT and M456A showed the Cu^{2+}-related catalytic wave at 250 mV in the presence

of exogenous Cu^{2+} added in the electrolyte (Fig. 8). This catalytic wave was previously proposed to be linked to an electron transfer pathway from the electrode to sCu bound in the M-rich domain and T1 Cu [23]. In contrast, the signal for direct O_2 reduction by M455L adsorbed on nanofiber-modified electrode disappeared in the presence of Cu^{2+} (Fig. 8B).

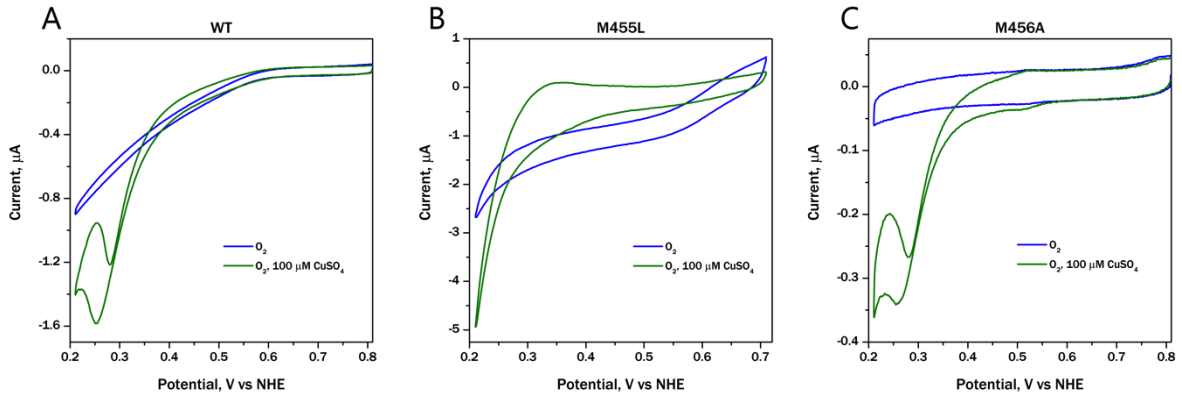


Fig. 8. *O_2 catalytic reduction by Tt-LAC WT (A), M455L (B) and M456A (C) adsorbed on graphite electrode (A and C) and carbon nanofiber-modified electrode (B) in the absence (blue lines) or presence of 100 µM $CuSO_4$ (green lines). 50 mM acetate buffer pH 5.6, sweep rate 5 mV.s^{-1}.*

It was recently discussed the flexibility of the M-rich domain in CueO-type LACs [28]. Bounding of sCu will certainly have an impact on the position of the M-rich domain, giving access to the substrate. Interestingly, an activation lag of around 100 s was observed with M456A in comparison with WT (Fig. 6D). It can be hypothesized a slow conformation change of M456A mutant upon Cu^{2+} addition which allows to recover the electron transfer pathway from ABTS to T1 Cu through the sCu. As shown in Fig. S4, a similar activation lag is observed with the double mutant. In contrast, the inhibition process observed with M455L and M455F is intriguing. It cannot be explained by protein denaturation as CD spectroscopy proved protein stability upon $CuSO_4$ addition (Fig. 2). Instead, data obtained with M455L and M455F clearly highlight that the presence of M as axial amino acid in the T1 redox site (M455) plays a key role in the activation process. The kinetic data of the double mutant, activation in the presence of $CuSO_4$ with a low $K_{1/2}$ however, would reflect some antagonist activation/inhibition of each single mutation. Whereas the related studies have focused on the role of methionines in the M-rich domain of CueO-like LACs, our work highlights that M-rich hairpin is not the only actor in Tt-LAC copper activation.

4. Conclusion

We have compared in this work the enzymatic activity of the laccase from *Thermus thermophilus* and two mutants in the vicinity of T1 Cu, obtained by directed mutagenesis. A multidisciplinary approach combining enzymatic assays, various spectroscopies, and electrochemistry has been used to obtain new insight in the properties of Tt-LAC. Our preliminary objective was to enhance the redox potential of the T1 Cu to improve the capability of O_2 catalytic reduction by the enzyme. Mutation of the methionine axial ligand into leucine residue induced an increase of 100 mV in the O_2 reduction potential. This result agrees with previously reported data for other LACs, underlining that the anodic shift of the T1 Cu redox potential by mutation of the methionine ligand into a less coordinating residue should be regarded as a general rule. However, the enzymatic activity for ABTS oxidation, a phenol representative, was drastically decreased. The catalytic current observed with the mutant immobilized on an electrode, was also greatly affected, negatively counterbalancing the positive effect on the redox potential. Nevertheless, mutation by random mutagenesis should allow in the future to increase the activity while maintaining a high redox potential for O_2 reduction. This strategy should be especially attractive for use of Tt-LAC in biotechnology, because its resistance to temperature should increase the overall stability thanks to a more compact structure.

The second objective of this work was to examine the effect of mutations in the T1 Cu vicinity on the activation of the enzyme by Cu^{2+}. Tt-LAC is a CueO-like protein. This family of enzymes is proposed to be involved in copper detoxification, and its *in vivo* role would be Cu^{+} oxidation and not phenol oxidation as usual LACs. Interestingly, the approach used in the current work, combining enzymatic assays in solution and electroenzymatic activity, allows to study both the phenol oxidase activity (ABTS assays in solution), and the cuprous oxidase activity (electrocatalytic wave in the presence of Cu^{2+}). Most studies in the literature evocate the presence of a methionine-rich domain in CueO-like proteins that can accommodate additional copper atoms. However, we showed recently by electrochemistry, that the deletion of the Met-rich domain in Tt-Lac did not decrease the cuprous oxidase activity [23]. Otherwise, a CueO-like enzyme was also identified in *Desulfovibrio* sp. A2 bacterium, showing Cu^{2+} typical activation, but lacking the M-rich domain [47]. The marked result obtained in this work confirms that the mechanism of Cu^{2+} activation of CueO-like protein is far from being understood. We effectively clearly showed that other residues than those in the M-rich domain have a role in the Cu^{2+}-activation process. Identification of the residues involved in copper detoxification will be required not only to understand the mechanism behind copper tolerance of microorganisms, but also to generate Cu^{+} sensor proteins, or to envision the development of Cu^{+} sensors.

Author's contributions

The author's responsibilities were as follows: RC designed the experimental study and analyzed biochemical data, XW carried out UV-Vis experiments, FB was in charge of EPR data analysis, MI was involved in the biochemical data analysis, IM and EL were involved in the electrochemistry analysis, EL prepared the manuscript. All the contributors reviewed the manuscript.

Author agreement

All authors have read this manuscript and approved to submit to your journal.

Declaration of competing interest

The authors declined any conflict of interest.

Acknowledgment

This work was supported by ANR (ENZYMOR-ANR-16-CE05- 0024). The authors are also grateful to the EPR facilities available at the French EPR network (IR CNRS 3443) and the Aix-Marseille University EPR centre. They thank Ahmed Zellat (BIP, Marseille, for ICP measurements), Dr Éric Durant (LISM, Marseille, for molecular biology), Pascale Infossi, Ludovica Quattrocchi (BIP, CNRS Marseille) for experimental assistance, and Dr Anne de Poulpiquet for fruitful discussion and critical reading of the manuscript.

References

1 Kaur K, Sharma A, Capalash N & Sharma P (2019) Multicopper oxidases: Biocatalysts in microbial pathogenesis and stress management. *Microbial. Res.* **222**, 1-13.

2 Guan Z-B, Luo Q, Wang H-R, Chen Y & Liao X-R (2018) Bacterial laccases: promising biological green tools for industrial applications. *Cell. Mol. Life Sci.s* **75**, 3569–3592.

3 Janusz G, Pawlik A, Swiderska-Burek U, Polak J, Sulej J, Jarosz-Wilkolazka A & Paszczynski A (2020) Laccase Properties, Physiological Functions, and Evolution. I*nt. J. Mol. Sci.* **21**, 966.

4 Theerachat M, Guieysse D, Morel S, Remaud-Siméon M & Chulalaksananukul W (2019) Laccases from marine organisms and their applications in the biodegradation of toxic and environmental pollutants: a review. *App. Biochem. Biotechnol.y* **187**, 583–611.

5 Ba S & Kumar VV (2017) Recent developments in the use of tyrosinase and laccase in environmental applications. *Criti. Revi.n Biotechnol.* **37**, 819–832.

6 Mano N & de Poulpiquet A. (2018) O_2 reduction in enzymatic fuel cells. *Chem. Rev.* **118**, 2392-2468.

7 Mazurenko I, Wang X, de Poulpiquet A & Lojou E (2017) H2/O2 enzymatic fuel cells: from proof-of-concept to powerful devices. *Sust. Energ. Fuels* **1**, 1475–1501.

8 Xiao X, Xia H, Wu R, Bai L, Yan L, Magner E, Cosnier S, Lojou E, Zhu Z & Liu A (2019) Tackling the challenges of enzymatic (bio)fuel cells. *Chem Rev* **119**, 9509–9558.

9 Mazurenko I, Monsalve K, Infossi P, Giudici-Orticoni M-T, Topin F, Mano N & Lojou E (2017) Impact of substrate diffusion and enzyme distribution in 3D-porous electrodes: a combined electrochemical and modelling study of a thermostable H2/O2 enzymatic fuel cell. *Energ. Environ. Sci.* **10**, 1966–1982.

10 Monsalve K, Mazurenko I, Gutierrez-Sanchez C, Ilbert M, Infossi P, Frielingsdorf S, Giudici-Orticoni MT, Lenz O & Lojou E (2016) Impact of carbon nanotube surface chemistry on hydrogen

oxidation by membrane-bound oxygen-tolerant hydrogenases. *ChemElectroChem* **3**, 2179–2188.

11 Valles M, Kamaruddin AF, Wong LS & Blanford CF (2020) Inhibition in multi copper oxidases: a critical review. *Catal. Sci. Technol.* **10**, 5386-5410.

12 Haque RU, Paradisi F & Allers, T (2020) Haloferax volcanii for biotechnology applications: challenges, current state and perspectives. *Appl. Microbiol. Biotechnol.* **104**, 1371-1382.

13 Jafari N, Rezaei S, Rezaie R, Dilmaghani H, Khoshayand MR & Faramarzi MA (2017) Improved production and characterization of a highly stable laccase from the halophilic bacterium Chromohalobacter salexigens for the efficient delignification of almond shell bio-waste. *Inter. J. Biol. Macromol.* **105**, 489-498.

14 Atalah J, Caceres-Moreno P, Espina G & Blamey JM (2019) Thermophiles and the applications of their enzymes as new biocatalysts. *Biores. Technol.* **280**, 478-488

15 Stanzione I, Pezzella C, Giardina P, Sannia G & Piscitelli A (2020) Beyond natural laccases: extension of their potential applications by protein engineering. *App. Microbiol. Biotechnol*. **104**, 915-924.

16 Mate DM & Alcalde M (2015) Laccase engineering: From rational design to directed evolution. *Biotechnol. Adv.* **33**, 25–40.

17 Zhang LL, Cui HY, Zou Z, Garakani TM, Novoa-Henriquez,C, Jooyeh B & Schwaneberg U (2019) Directed Evolution of a Bacterial Laccase (CueO) for Enzymatic Biofuel Cells. *Ang. Chem. Inter. Ed.* **58**, 4562-4565.

18 Liu Y, Ye M, Lu Y, Zhang X & Li G (2011) Improving the decolorization for textile dyes of a metagenome-derived alkaline laccase by directed evolution. *App. Microbiol. Biotechnol.* **91**, 667–75.

19 Mate DM, Gonzalez-Perez D, Falk M, Kittl R, Pita M, Lacey ALD, Ludwig R, Shleev S & Alcalde M (2013) Blood tolerant laccase by directed evolution. *Chemi. Biol.* **20**, 223–231.

20 Sheng S, Jia H, Topiol S & Farinas E (2016) Engineering CotA Laccase for Acidic pH Stability Using Bacillus subtilis Spore Display. *J. Microbiol. Biotechnol.* **27**.

21 Miyazaki K (2005) A hyperthermophilic laccase from Thermus thermophilus HB27. *Extremophiles* **9**, 415–425.

22 Serrano-Posada H, Valderrama B, Stojanoff V & Rudiño-Piñera E (2011) Thermostable multicopper oxidase from Thermus thermophilus HB27: crystallization and preliminary X-ray diffraction analysis of apo and holo forms. *Acta Crystallographica Section F* **67**, 1595–1598.

23 Hitaishi VP, Clément R, Quattrocchi L, Parent P, Duché D, Zuily L, Ilbert M, Lojou E & Mazurenko I (2020) Interplay between orientation at electrodes and copper activation of Thermus thermophilus laccase for O2 reduction. *J. Am. Chem. Soc.* **142**, 1394–1405.

24 Roberts S, Wildner G, Grass G, Weichsel A, Ambrus A, Rensing C & Montfort W (2003) A labile regulatory copper ion lies near the T1 copper site in the multicopper oxidase CueO. *J. Biol. Chem.* **278**, 31958–63.

25 Singh S., Roberts S., McDevitt S., Weichsel A., Wildner G., Grass G., Rensing C & Montfort W (2011) Crystal structures of multicopper oxidase CueO bound to copper(I) and silver(I), Functional role of a methionine-rich sequence. *J. Biol. Chem* **286**, 37849-37857.

26 Cortes L, Wedd A. & Xiao Z. (2015) The functional roles of the three copper sites associated with the methionine-rich insert in the multicopper oxidase CueO from *E. coli*. *Metallomics* **7**, 776-785.

27 Wang H., Liu X., Zhao J., Yue Q., Yan Y., Gao Z., Dong Y., Zhang Z., Fan Y., Tian J., Wu N. & Gong Y. (2018) Crystal structures of multicopper oxidase CueO G304K mutant: structural basis of the increased laccase activity. *Sci. Reports* **8**, 14252.

28 Borges P., Brissos V., Hernandez G., Masgrau L., Lucas M., Monza E., Frazao C., Cordeiro T. & Martins L. (2020) Methionine-rich loop of multicopper oxidase McoA follows open-to-close transitions with a role in enzyme catalysis. *ACS Catal.* **10**, 7162-7176.

29 Adachi T., Kitazumi Y., Shirai O., Kawano T., Kataoka K. & Kano K. (2020) Effects of elimination of a helix regions on direct electron transfer-type bioelectrocatalytic properties of copper efflux oxidase. *Electrochem.* **88**, 185-189.
30 Osipov E, Polyakov K, Kittl R, Shleev S, Dorovatovskii P, Tikhonova T, Hann S, Ludwig R & Popov V (2014) Effect of the L499M mutation of the ascomycetous Botrytis aclada laccase on redox potential and catalytic properties. *Acta crystallographica Section D, Biological crystallography* **70**, 2913–23.
31 Zhu Y, Zhang Y, Zhan J, Lin Y & Yang X (2019) Axial bonds at the T1 Cu site of Thermus thermophilus SG0.5JP17-16 laccase influence enzymatic properties. *FEBS Open Bio* **9**, 986–995.
32 Jeong J-Y, Yim H-S, Ryu J-Y, Lee HS, Lee J-H, Seen D-S & Kang SG (2012) One-step sequence- and ligation-independent cloning as a rapid and versatile cloning method for functional genomics studies. *App. Environ. Microbiol.* **78**, 5440–5443.
33 Kelley L, Mezulis S, Yates C, Wass M & Sternberg M (2015) The Phyre2 Web Portal for Protein Modeling, Prediction and Analysis. *Nat. protocols* **10**, 845–58.
34 Stoll S & Schweiger A (2006) EasySpin, a comprehensive software package for spectral simulation and analysis in EPR. *J. Magn. Resonance* **178**, 42–55.
35 Poulpiquet A de, Marques-Knopf H, Wernert V, Giudici-Orticoni MT, Gadiou R & Lojou E (2014) Carbon nanofiber mesoporous films: efficient platforms for bio-hydrogen oxidation in biofuel cells. *Phys. Chem. Chem. Phys.* **16**, 1366–1378.
36 Durao P, Chen Z, Fernandes A, Hildebrandt P, Murgida D, Todorovic S, Pereira M, Pinho Melo E & Martins L (2008) Copper incorporation into recombinant CotA-laccase from Bacillus subtilis: Characterization of fully copper loaded enzymes. *J. Biol. Inorg. Chem.* **13**, 183–93.
37 Gounel S, Rouhana J, Stines-Chaumeil C, Cadet M & Mano N (2016) Increasing the catalytic activity of Bilirubin oxidase from Bacillus pumilus: Importance of host strain and chaperones proteins. *J. Biotechnol.* **230**, 19–25.
38 Samak N, Hu J, Wang K, Guo C & Liu C (2018) Development of a novel micro-aerobic cultivation strategy for high potential CotA laccase production. *Waste Biomass Valor*. **9**, 369-377.
39 Galli I, Musci G. & Bonaccorsi di Patti M (2004) Sequential reconstitution of copper sites in the multicopper oxidase CueO. *J. Biol. Inorg. Chem.* **9**, 90-95.
40 Durao P, Chen Z, Silva C, Soares C, Pereira M, Todorovic S, Hildebrandt P, Bento I, Lindley P & Martins L (2008) Proximal mutations at the type 1 copper site of CotA laccase: Spectroscopic, redox, kinetic and structural characterization of I494A and L386A mutants. *Biochem. J.* **412**, 339–46
41 Solomon EI, Heppner DE, Johnston EM, Ginsbach JW, Cirera J, Qayyum M, Kieber-Emmons MT, Kjaergaard CH, Hadt RG & Tian L (2014) Copper active sites in biology. *Chem. Rev.* **114**, 3659–3853.
42 Bennett B & Kowalski JM (2015) EPR methods for biological Cu(II): L-band CW and NARS. *Methods Enzymol.* **563**, 341–361.
43 Bello M, Correa-Basurto J & Rudiño-Piñera E (2014) Simulation of the cavity-binding site of three bacterial multicopper oxidases upon complex stabilization: Interactional profile and electron transference pathways. *J. Biomol. Struct. Dyn.* **32**.
44 Marcus RA (1956) On the Theory of Oxidation-Reduction Reactions Involving Electron Transfer. *J. Chem. Phys.* **24**, 966–978.
45 Durao P, Bento I, Fernandes AT, Melo EP, Lindley PF & Martins LO (2006) Perturbations of the T1 copper site in the CotA laccase from Bacillus subtilis: structural, biochemical, enzymatic and stability studies. *J. Biol. Inorg. Chem.* **11**, 514.
46 Solano F, Lucas-Elio P, López-Serrano D, Fernández E & Sanchez-Amat A (2001) Dimethoxyphenol oxidase activity of different microbial blue multicopper proteins. *FEMS Microbiol. Letters* **204**, 175–81.
47 Mancini S, Kumar R, Mishra V & Solioz M (2017) Desulfovibrio DA2_CueO is a novel multicopper oxidase with cuprous, ferrous and phenol oxidase activity. *Microbiol.* **163**, 1229–1236.